Oligomerization of β-amyloid of the Alzheimer's and the Dutch-cerebral-haemorrhage types

Aneet K. SIAN*, Emma R. FREARS*, Omar M. A. EL-AGNAF*, Bhroma P. PATEL*, Maria F. MANCA*, Giuliano SILIGARDI†, Rohanah HUSSAIN† and Brian M. AUSTEN*[1]

*Department of Surgery, St. George's Hospital Medical School, Cranmer Terrace, London SW17 ORE, U.K., and †Department of Pharmacy, King's College, Franklin–Wilkins Building, 150 Stamford Street, London SE1 8WA, U.K.

A novel ELISA has been developed which detects oligomerization of β-amyloid (Aβ). Oligomerization, fibrillization and neurotoxicity of native Aβ associated with Alzheimer's disease (AD) type has been compared with E22Q Aβ (amyloid β-protein containing residues 1–40 with the native Glu at residue 22 changed to Gln) implicated in Dutch cerebral haemorrhage disease. Solutions of Aβ rapidly yield soluble oligomers in a concentration-dependent manner, which are detected by the ELISA, and by size-exclusion gel chromatography. Conformational changes from disordered to β-sheet occur more slowly than oligomerization, and fibrils are produced after prolonged incubation. The E22Q Aβ oligomerizes, changes conformation and fibrillizes more rapidly than the native form and produces shorter stubbier fibrils. Aged fibrillar preparations of E22Q Aβ are more potent than aged fibrils of native Aβ in inducing apoptotic changes and toxic responses in human neuroblastoma cell lines, whereas low-molecular-mass oligomers in briefly incubated solutions are much less potent. The differences in the rates of oligomerization of the two Aβ forms, their conformational behaviour over a range of pH values, and NMR data reported elsewhere, are consistent with a molecular model of oligomerization in which strands of Aβ monomers initially overcome charge repulsion to form dimers in parallel β-sheet arrangement, stabilized by intramolecular hydrophobic interactions, with amino acids of adjacent chains in register.

Key words: apoptosis, ELISA, fibril, parallel β-sheet, toxicity.

INTRODUCTION

Alzheimer's disease (AD) is a progressive degenerative disease of the brain characterized by loss of cognitive function (dementia), selective neuronal death and the abnormal formation of neuritic and core plaques throughout the cerebral cortex, predominating in the hippocampus and temporal lobe cortex, and around the blood vessels of the meninges and cerebral cortex. Deposits in brain are associated with reactive microglia, astrogliosis and neuronal loss. The major component of AD amyloid deposits is a 39–43-residue amyloid β (Aβ) peptide, which is produced as a cleavage product of a much larger transmembrane glycoprotein, encoded by the amyloid-precursor-protein (APP) gene on chromosome 21 [1].

A mutated form of Aβ is also deposited in a rare form of amyloidosis known as hereditary cerebral haemorrhage with amyloidosis Dutch type (HCHWA-D), a disease that typically manifests itself with recurring strokes and dementia. In a pathological study, both HCHWA-D and AD showed compact cerebral amyloid angiopathy (CAA) with Aβ deposits in arterial/arteriolar media and concomitant smooth-muscle cell loss, whereas only HCHWA-D CAA featured severe involvement of larger arteries and arterioles, with a single or double rings of radial deposited Aβ [2]. In contrast with AD, the neuropil of HCHWA-D patients showed diffuse rather than senile plaques, which were not associated with neuronal loss [3]. The toxicity of the HCHWA-D form of Aβ toward neurons has not previously been reported. HCHWA-D is an autosomal dominant condition associated with a point mutation at codon 693 of the gene for βAPP, which leads to the substitution of glutamic acid at position 22 of Aβ with glutamine. The mutation does not alter the ratio of secreted Aβ to p3 (peptides comprising the C-terminal residues 17–40 or 17–42 of Aβ), nor the stability of the secreted Aβ and p3 peptides, but increases the biosynthesis of Aβ peptides with N-termini of Asp^{1}, Val^{18} and Phe^{19} [4]. Why this single mutation leads to the extreme severity of the vascular pathology, hallmark of HCHWA-D, as well as the absence of senile plaques in the neuropil, is so far not clear.

A central question in the etiology of AD and HCHWA-D is the mechanism(s) by which soluble Aβ monomers are converted into fibrillar deposits. This question is particularly relevant because Aβ fibres, unlike soluble monomers, are neurotoxic *in vitro* [5–7] and associated with damaged neuropil *in vivo* [8]. Using optical microscopy, ultracentrifugation and electrophoresis, it was shown that only aggregated forms of Aβ peptides containing the hydrophobic region 25–35 were toxic to primary neurons [5]. Upon reversal of aggregation, neurotoxicity disappeared.

There is disagreement over the precise structure of the neurotoxic forms of Aβ. Protofibrils, distinguished from mature fibrils by their appearance under the electron microscope, were reported as toxic as mature fibrils [9]. Low-molecular-mass oligomers induced toxicity in long-term neuronal cultures, but were less toxic than fibrils [9]. Protofibrils and fibrils, but not low-molecular-mass oligomers, alter the electrical activity of neurons, and it has been suggested that preclinical and early progression

Abbreviations used: Aβ, amyloid β-protein containing residues 1–40; p3, peptides comprising the C-terminal residues 17–40 or 17–42 of Aβ; AD, Alzheimer's disease; APP, amyloid precursor protein; HCHWA-D, hereditary cerebral haemorrhage with amyloidosis Dutch type; CAA, cerebral amyloid angiopathy; Fmoc, fluoren-9-ylmethoxycarbonyl; NTA4, a peptide containing the ten N-terminal residues of β-amyloid; E22Q Aβ, amyloid β-protein containing residues 1–40 with the native Glu at residue 22 changed to Gln; MEM, minimal essential medium; MTT, 3-(4,5-dimethylthiazol-2-yl)-2,5-diphenyltetrazolium bromide; QLS, quasi-light-scattering spectroscopy; ACTH, adrenocorticotrophic hormone.

[1] To whom correspondence should be addressed (e-mail sghk200@sghms.ac.uk).

of AD is driven by accumulation of oligomeric intermediates prior to the assembly of fibrils [9]. In contrast, some authors suggest that soluble Aβ dimers, which purportedly survive SDS treatment [10], are highly toxic to neuronal cultures [11]. Fluorescence measurements indicate that Aβ dimers may be stable at very low concentrations [12], and Western blotting has suggested that Aβ dimers are formed in the brains of AD patients before fibrillary tangles [13].

In order to define the structural and oligomeric changes that take place in Aβ solutions in more detail, a novel ELISA assay that monitors the formation of oligomers from monomers has been developed. We have correlated the changes found in solutions of Aβ peptides by ELISA with changes observed by gel filtration and CD. Finally, the apopototic and toxic changes induced by Aβ peptides incubated for different times have been determined. As the Q22E mutation appears to produce quite a distinct phenotype, we have compared the properties of Q22E 1–40 with native Aβ.

EXPERIMENTAL

Preparation of aggregated 'aged' solutions of Aβ peptides

Aβ peptides were synthesized using fluoren-9-ylmethoxycarbonyl (Fmoc) chemistry on a Millgen 9050 synthesizer (PE Biosystems, Warrington, Cheshire, U.K.) by an optimized protocol [14], purified by acetonitrile gradients on HPLC on Vydac C_8 columns in 0.1 % (v/v) trifluoroacetic acid, and freeze-dried. Aβ peptides were shown to be homogeneous by MS. Aβ peptides were dissolved first in sterilized distilled water, then a 10 % volume of sterilized 1 M Tris/HCl, pH 7.4, was added to give a final peptide concentration of 1.16 mM. These solutions were aged by incubating them at 37 °C.

Preparation of the biotinylated antibody

Biotinamidohexanoate *N*-hydroxysuccinimide (Sigma–Aldrich, Poole, Dorset) (20 μl of a 10 mg/ml solution in DMSO) was added to anti-NTA4, an affinity-purified antibody to the N-terminal ten residues of Aβ coupled to BSA [15] in 0.1 M sodium borate, pH 8 (0.5 ml at 1 mg/ml), and incubated at 24 °C for 4 h. Ammonium chloride (20 μl of 1 M) was added, and incubation continued for 10 min. The mixture was desalted on a Sephadex G-25 column in PBS to remove excess uncoupled biotin. The biotinylated antibody was stored at −20 °C.

An ELISA to measure oligomers

An ELISA plate was coated with 5 μg/ml of non-biotinylated anti-NTA4 antibody (100 μl/well) in PBS/0.01 % (w/v) sodium azide at 4 °C for 24 h, washed twice with blocking buffer (PBS/1 % BSA/0.05 % Tween, pH 7.4), and incubated with blocking buffer for 1 h at room temperature. Peptides incubated in 0.1 M Tris were diluted to 18 nM in blocking buffer, and 100μl added to each well. The plate was incubated at 37 °C for 2 h.

After washing four times with blocking buffer, biotinylated anti-NTA4 diluted 1 to 500 in blocking buffer (100 μl) was added, and incubated at 37 °C for 1.5 h. Wells washed three times with blocking buffer were incubated with peroxidase–avidin (Sigma) (1:1000 in blocking buffer) (100 μl) at 37 °C for 1.5 h, washed three times with PBS/1 % (w/v) BSA/0.05 % (v/v) Tween, pH 7.4, and once with PBS/0.05 % (v/v) Tween, before adding substrate for peroxidase (Europa Ltd., Wicken, Ely, Cambs., U.K.) (100 μl), developing for about 5 min before adding 1 M H_2SO_4 (100 μl) and reading at 450 nm.

Size-exclusion chromatography

Aliquots (20 μl) of freshly prepared or incubated solutions of Aβ peptides at 1.16 mM in 0.1 M Tris/HCl, pH 7.4, were loaded on a Superdex 75 gel-filtration column (10 cm × 270 mm) in 0.1 M Tris/HCl, pH 7.4, with a flow rate of 0.5 ml/min. Eluate was monitored at 215 nm.

CD

Spectra were recorded with nitrogen-flushed JASCO J720 and J600 spectropolarimeters using 4 s time constant, 10 nm/min scan speed and a spectral bandwidth of 2 nm. Both spectropolarimeters were calibrated with ammonium D-camphor-10-sulphonate. Quartz cells of 0.02 cm and 1 cm were used for measurements in the far-UV (185–250 nm) and near-UV (250–350 nm) regions respectively. CD spectra were reported as:

$$\triangle\epsilon = \epsilon_L - \epsilon_R \ (M^{-1} \cdot cm^{-1})$$

where $\triangle\epsilon$ is the difference between the molar absorbance of left circularly polarized light (ϵ_L) and the molar absorbance of right circularly polarized light (ϵ_R) and is based upon an average molecular mass per amino acid of 113.

Electron microscopy

Samples of precipitated peptides aged at 1.16 mM (10 μl) were fixed with glutaraldehyde, stained with uranyl acetate and examined on a Zeiss 900 transmission electron microscope [16].

Cell culture

SH-SY5Y cells (European Collection of Cell Cultures, Porton Down, Salisbury, Wilts., U.K.) were cultured in Dulbecco's minimal essential medium (MEM)/Nutrient Mix F-12 (1:1, v/v) (Gibco BRL) containing 10 i.u. of penicillin/ml and 100 μg/ml streptomycin, 15 % (v/v) foetal-calf serum, 1 % non-essential MEM amino acid supplement, and 2 mM freshly prepared glutamine at 37 °C in a humidified incubator with CO_2/room air (1:19).

Cytotoxicity assay

The cytotoxicity of Aβ peptides was assessed by measuring cellular redox activity. Cells were plated at a density of 7500 cells/well in 96-well plates in 100 μl of fresh medium. After 24 h the medium was replaced with 100 μl of OPTI-MEM (Gibco BRL) serum-free medium and aged or fresh Aβ peptides diluted in OPTI-MEM added. The positive control contained 15 μM camptothecin (Sigma). Cells were incubated at 37 °C in 5 % CO_2 for 48 h. Medium was replaced with RPMI-1640 without Phenol Red (Sigma) (100 μl), 25 μl of 3-(4,5-dimethylthiazol-2-yl)-2,5-diphenyltetrazolium bromide (MTT) (Sigma) (5 mg/ml) added to each well and the plate incubated at 37 °C for 3 h [17]. The plate was centrifuged for 5 min at 137 ***g*** (Sorvall RT 6000D centrifuge) and the medium/MTT solution removed. Propan-1-ol (100 μl) was added and the plate shaken for 60 min and read at 570 nm.

Apoptosis assay

Apoptosis was detected by using an annexin V/propidium iodide (Vybrant™ Apoptosis Assay Kit), and mitochondrial tracker (CMXRos/Sytox; Molecular Probes, Eugene, OR, U.S.A.). An eight-well chambered coverglass (Nalge Nunc International,

Naperville, IL, U.S.A.) was seeded with 0.45 ml of SH-SY5Y cells at 290 000 cells/ml and incubated for 20 h. Medium was replaced with OPTI-MEM with aged or fresh peptide solutions. Positive controls contained 15 or 50 μM camptothecin, or 100 μM H_2O_2. Chambers were incubated for 9 h at 37 °C. Adhering cells were washed twice with ice-cold PBS and Annexin-Binding Buffer (Molecular Probes) (100 μl) added. Alexa 488 annexin V (5 μl) and propidium iodide (1 μl, 100 μg/ml) (Molecular Probes) were added and cells incubated in the dark for 15 min. Alternatively, cells were incubated for 20 min at 37 °C with Mitochondrial tracker at 0.11 μg/ml and Sytox at 0.1 μM. Unbound reagents were washed out with ice-cold Annexin Binding Buffer or PBS, and cells were inspected by confocal microscopy on a Carl Zeiss laser scanning microscope, using a narrow pass 515–565 nm filter and 488 irradiation or a > 695 nm filter with 546 irradiation.

RESULTS

Oligomer formation detected by ELISA

An ELISA was developed to detect soluble oligomers of Aβ. Solutions of both Aβ and E22Q Aβ incubated at 1.16 mM at pH 7.4 in 0.1 M Tris/HCl for up to 3 h, and then immobilized on to a non-biotinylated form of the antibody anti-NTA4, showed a rapid increase in binding to the biotinylated antibody by the increase in absorbance in the ELISA assay (Figure 1). No increase in binding of biotinylated anti-NTA4 was found in control 1.16 mM pre-incubated solutions of the N-terminal ten-residue peptide of Aβ. The rate of increase was more rapid for E22Q Aβ than for the native sequence. Preincubation of the

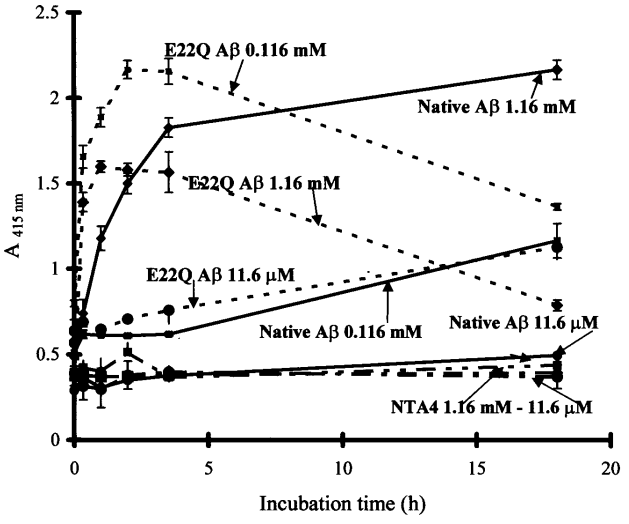

Figure 1 Oligomerization of Aβ peptides measured by ELISA

Solutions of native Aβ (continuous lines) or E22Q Aβ (variously broken lines) in 0.1 M Tris/HCl, pH 7.4, at 1.16 mM, 0.116 mM and 11.6 μM were incubated at 37 °C, diluted to 18 nM, and incubated on an ELISA plate already coated with immobilized anti-NTA4 antibody. Additional epitopes formed by oligomerization during the pre-incubation step were measured by subsequent binding to a biotinylated sample of anti-NTA4. The plots of negative controls containing the ten-residue peptide NTA4 incubated at 1.16 mM, 0.116 mM and 11.6 μM, are also shown (bottom three curves). S.E.M. values for assays performed in triplicate are shown for each point as bars above and/or below the mean. The mid-range of the assay for 18 h-oligomerized native Aβ was 0.9 nM. At 0.9 nM concentration, the within-assay variance was 5.7%. A day-to-day variance of 5.2% at 0.9 nM was found in seven assays calibrated with standard solutions of Aβ incubated in 0.1 M Tris/HCl, pH 7.4, at 1.16 mM for 18 h, diluted to 18 nM in blocking buffer, divided into aliquots and stored at −20 °C.

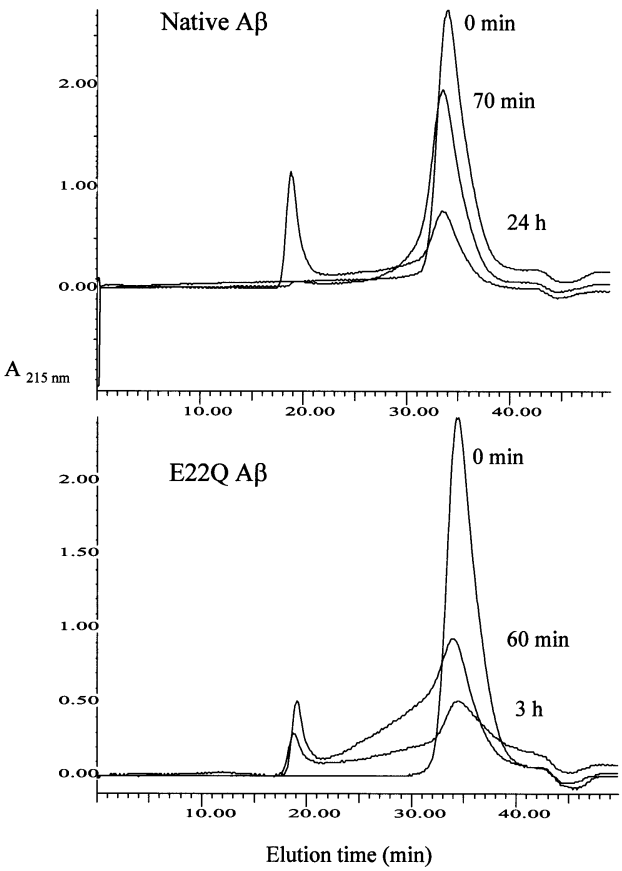

Figure 2 Size-exclusion chromatography of Aβ oligomers

Elution profiles of samples of solutions of native or E22Q Aβ pre-incubated at 1.16 mM in 0.1 M Tris, pH 7.4, at 37 °C for the times shown.

Table 1 Elution of proteins and peptides of known molecular mass from Superdex 75

Protein	Molecular mass (kDa)	Elution time (min)
BSA	68	22.7
Porcine lipotropin	9.9	29.3
Bovine aprotinin	6.5	53.4
Human ACTH	4.5	39.4
Human neuropeptide Y	4.2	64.0
MBP-TET peptide*	3.4	39.7
Tram peptide†	2.1	40.0
E22Q Aβ	4.3	34.6
Native Aβ	4.3	34.6

* A peptide containing the sequence YGGRASDYKSAHKGFKQYIKANSKFIGITE.
† A peptide of the sequence LDKINRRMHFSKTKHSC.

E22Q Aβ solutions for longer than 3 h gave a decrease from maximum response, and precipitates formed, which were shown by electron microscopy to contain fibrils (see below). E22Q Aβ preincubated at 0.116 mM produced soluble oligomers more slowly than at 1.16 mM, and reached a higher maximum value, possibly because fewer fibrils were formed at the lower concentration. In contrast, the increase in binding of biotinylated

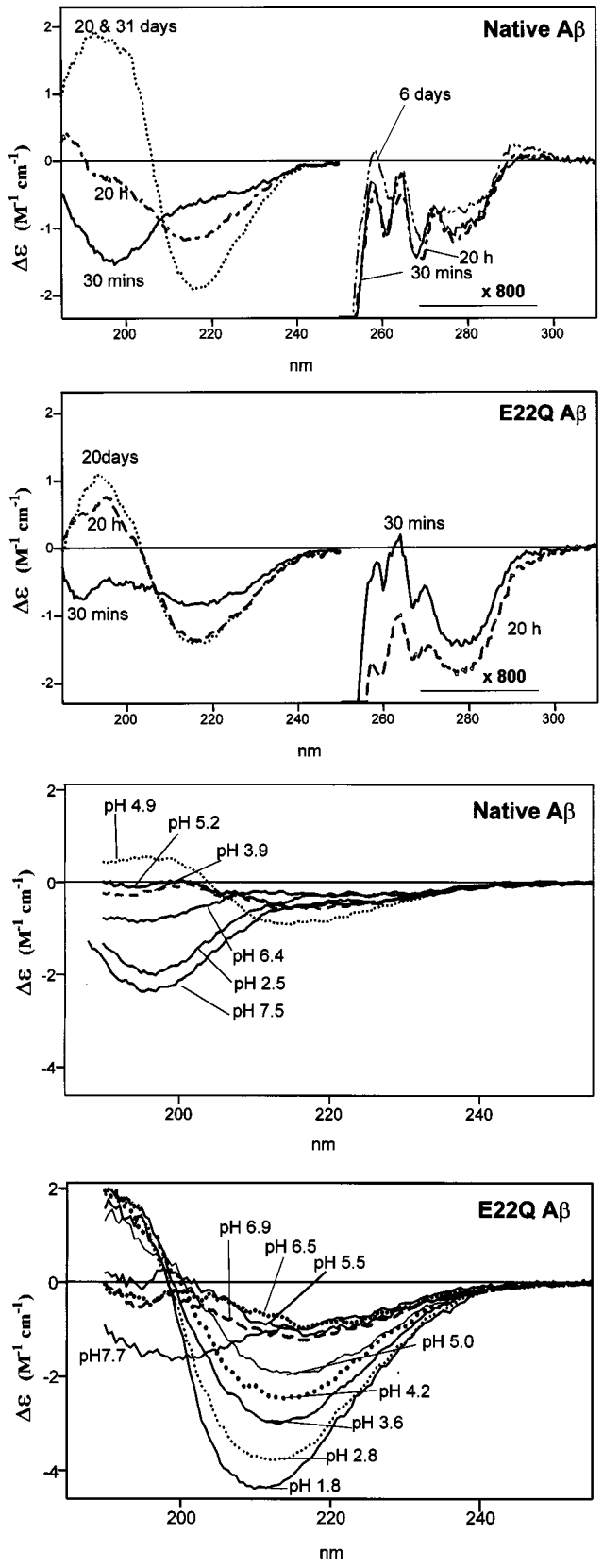

Figure 3 CD of Aβ peptide solutions

Top two panels: time-induced changes in the conformation of Aβ peptides. CD spectra of native (top) or E22Q (below) Aβ pre-incubated at 1.16 mM in 0.1 M Tris/HCl, pH 7.4, at 37 °C for either 30 min (continuous lines), 20 h (broken lines), 20 days (dotted lines) and 31 days (dotted line), then diluted 10-fold with water just prior to measurement. Bottom two panels: pH-induced changes in the conformations of Aβ peptides. CD spectra of fresh native (top) and E22Q (below) Aβ solutions in 10 mM Tris/HCl as a function of pH. The pH titration was carried out in a stepwise manner from pH 7.5 and pH 7.7 respectively by addition of aliquots of HCl. The pH was measured just before recording the spectra, and each spectrum obtained is shown marked with the pH value recorded. Sample at pH 1.8 (Figure 3, bottommost panel) was incubated for 25 h at pH 1.8 before recording spectra.

anti-NTA4 to soluble oligomers formed in preincubated solutions of native Aβ was less than with E22Q, and no precipitate was visible up to 24 h of incubation. Increases of binding to biotinylated anti-NTA4 of native Aβ preincubated at 0.116 mM and 11.6 μM were much less than with the same concentrations of E22Q Aβ. Over an 18 h incubation, about three times the amount of soluble oligomers, as judged by increase in binding to biotinylated NTA4, were produced by the E22Q mutant incubated at 0.116 mM than at 11.6 μM, whereas binding to biotinylated NTA4 caused by native Aβ oligomers produced at 11.6 μM concentration was about 4% of the binding produced at 1.16 mM.

Size-exclusion chromatography

Changes in the state of oligomerization of the Aβ peptides were also examined by size-exclusion chromatography on Superdex 75 (Figure 2). Fresh solutions of the Aβ peptides were eluted in one symmetrical peak at 34.6 min. Between 10 and 70 min of preincubation at 37 °C in 0.1 M Tris/HCl, pH 7.4, produced changes in the elution profiles. The major peaks were eluted slightly earlier (33.2 min) and shoulders appeared before the main peak. After 60 min preincubation for E22Q Aβ or 24 h for native Aβ, a second peak appeared at the flow-through volume (19 min). Attempts to calibrate the Superdex column with proteins and peptides of known molecular mass were not satisfactory (Table 1). The elution times of the fresh Aβ peptides were between those of adrenocorticotrophic hormone (ACTH; 4.5 kDa; 39.4 min) and lipotropin (9.4 kDa; 29.3 min) and might indicate that non-incubated Aβ was behaving as a peptide of 6.5 kDa. However, both neuropeptide Y (4.2 kDa) and aprotinin (6.4 kDa) were not eluted as expected from their molecular mass (see Table 1).

CD

CD spectroscopy of solutions of the Aβ peptides preincubated at 1.16 mM and then diluted 10-fold immediately before measurement are shown (Figure 3). Substantial differences were observed in the conformational behaviour of both peptides as a function of incubation time and pH. The rates of changes from mainly random coil to conformations of the β-sheet type were more than one order of magnitude different, with no further changes being observed after 20 days of incubation for native Aβ, or 20 h for E22Q Aβ. The changes taking place in the UV region between 250 and 290 nm during incubation were significantly more enhanced in E22Q Aβ than in native Aβ (Figure 3, top two panels).

The titration from pH 7.0 to 2.0, and the reverse titration from pH 2.0 to 7.0, revealed interesting CD spectra that differentiate and discriminate between the two Aβ forms. Both peptides showed random-coil-to-β-sheet transitions on lowering the pH from 7.0 to 4.0, by 0.5 pH unit in a stepwise manner. However, below pH 4.0, native Aβ 1–40 revealed an almost reversible β-sheet–random-coil transition, whereas E22Q showed further random-coil–β-sheet transitions. At pH 1.8 this transition took 24 h to stabilize (Figure 3, bottom two panels; plot marked 'pH

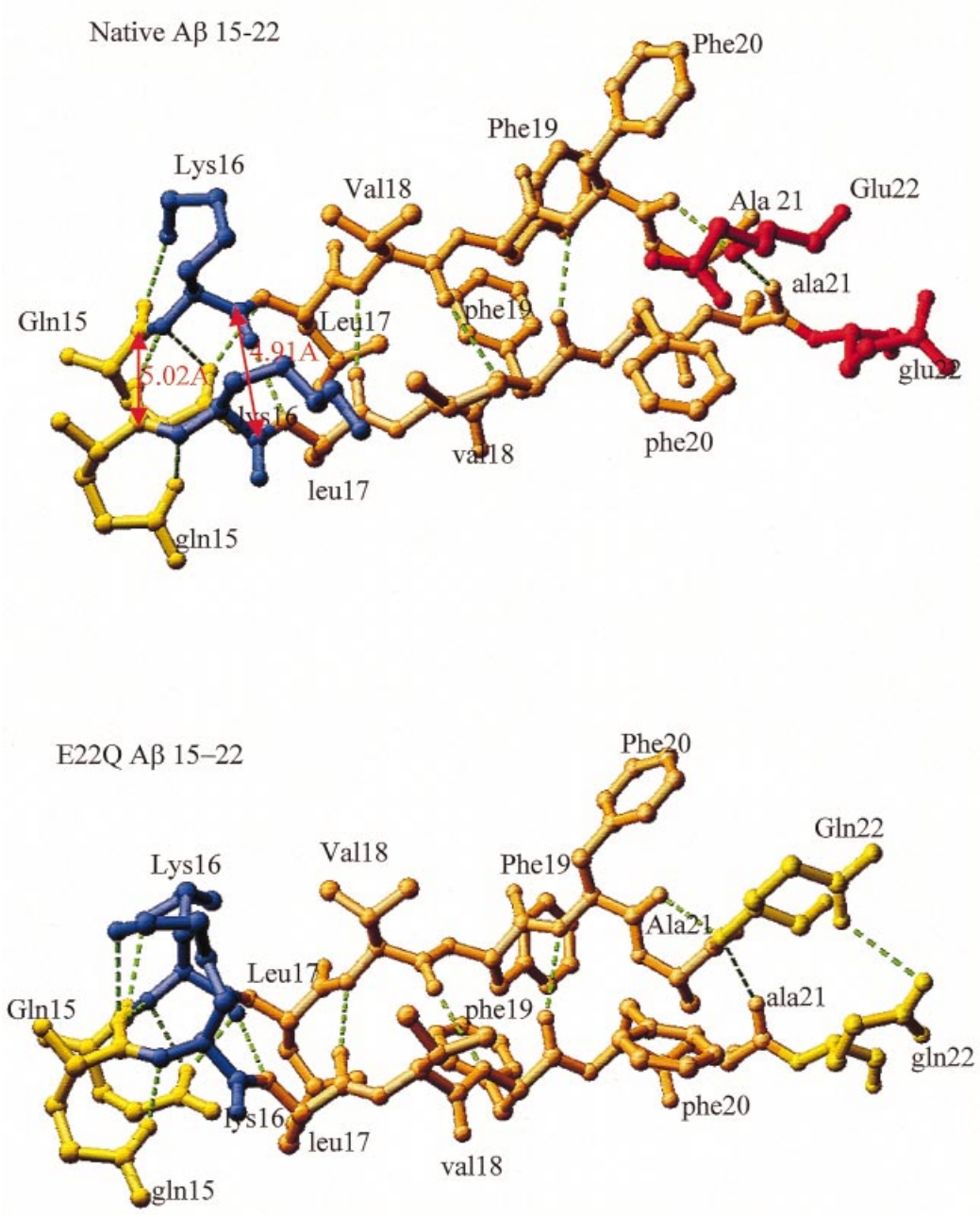

Figure 4 Energy-minimized molecular models of residues 15–22 of native and E22Q Aβ

Two strands of native or E22Q Aβ are shown modelled on Swiss-Prot PDB viewer in a parallel β-sheet arrangement, with the residues in register. Colour coding: broken lines, intermolecular hydrogen bonding; red, Glu^{22}; blue, Lys^{16}; yellow, Gln residues; brown, hydrophobic residues. Distances shown are measured between the carbonyl carbon atoms of the Gln^{15} residues and between the Lys^{16} residues.

1.8'). The rate of adoption of β-sheet at pH 2.8 was more than the rate of change monitored at pH 7.4.

Molecular modelling

Energy-minimized molecular models of dimeric sequences of residues 15–22 in the native and E22Q sequences were produced on Swiss PDB viewer. The model (Figure 4) indicated that hydrophobic interactions between the side chains in this region could be maximized by a parallel arrangement in which the β-strands were held together by hydrogen bonding between the peptide bonds, with amino acid residues on each strand in register.

Electron microscopy

Prolonged incubation of several hours for E22Q and 1 week for native Aβ yielded precipitated material. Precipitates produced from 3-week incubations were harvested, and subjected to electron microscopy. The results showed that the fibrils pro-

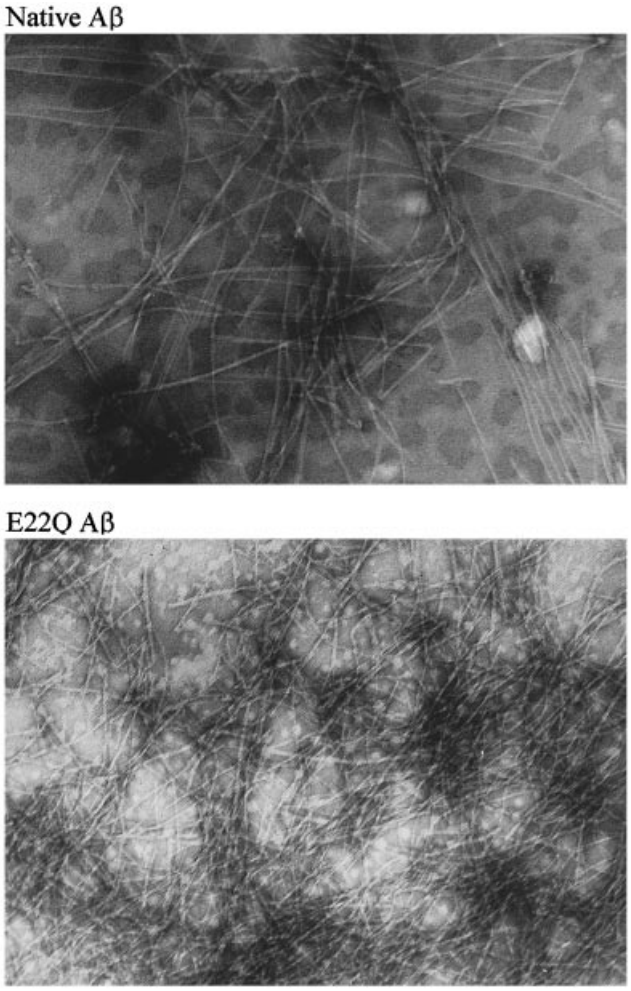

Figure 5 Transmission electronmicrographs of native and E22Q Aβ fibrils

Solutions of native or E22Q Aβ 1.16 mM were aged for 3 weeks at 37 °C in 0.1 M Tris/HCl, pH 7.4, and the precipitates fixed, stained, and examined on a Zeiss 900 transmission electron microscope. Magnification is $\approx 100\,000\times$.

duced from native Aβ were longer and thinner than those produced from E22Q Aβ (Figure 5).

Cytotoxic effect of aged and fresh βA4 peptides

The results obtained by ELISA (Figure 1) and size-exclusion chromatography (Figure 2) showed that native and E22Q peptides incubated at 1.16 mM for 1 h produced soluble oligomers. Several hours of incubation produced fibrillar forms of E22Q Aβ, whereas several days of incubation were required to fibrillize native Aβ. We then sought to find out which forms of the peptides were toxic to neuronal cells by finding out what periods of incubation time were required to produce high toxicity.

Human dopaminergic neuroblastoma SHSY-5Y cells were exposed to freshly prepared, 1-h- or 3-week-incubated solutions of E22Q Aβ and native Aβ. Camptothecin was used as a positive control. After incubation for a further 2 days, cell viability was evaluated using the MTT assay and compared with that of negative control cells incubated without peptide. Fresh native Aβ was much less toxic than fresh E22Q Aβ, whereas both solutions that had been incubated for 3 weeks showed considerable toxicity, even at concentrations below 1 μM (Figure 6A). At the highest concentrations, fresh E22Q Aβ was as toxic as aged E22Q Aβ. In contrast, there were no significant differences between toxicities of fresh solutions and those incubated at 1.16 mM for 1 h (Figure 6B); both incubates were equally toxic at high concentrations.

Apoptosis induced by Aβ peptides

In order to explore the differences between the two Aβ peptides further, SHSY-5Y cells were exposed to fibrils of native and E22Q Aβ for 10 h. Preparations of E22Q Aβ aged for 3 weeks completely ablated the mitochondrial membrane potential at 11.6 μM and 2.3 μM (Figures 7E and 7G). Aged native Aβ was also completely effective at 11.6 μM (Figure 7A), but only partly effective at 2.3 μM (Figure 7C). In contrast, freshly made solutions had little effect on mitochondrial potential (compare treated cells in Figures 7B, 7D, 7F and 7H with control cells in Figure 7I). Extensive staining of nuclei with Sytox was apparent only in cells treated with H_2O_2 (Figure 7L) or 50μM camptothecin (Figure 7J). No nuclear staining was seen in cells treated with 15 μM camptothecin. Most (90 %) of the cells treated with E22Q Aβ stained with annexin V (Figure 7N), and about 20 % also stained with propidium iodide. About 40 % of the cells exposed to native Aβ stained with annexin V (Figure 7M), with about 10 % staining with propidium iodide. Cells treated with camptothecin (15 μM) are shown in Figure 7(O) and control untreated cells in Figure 7(P).

DISCUSSION

It has been suggested that the toxic forms of Aβ are relatively soluble dimers that might do some of the damage by forming flickering deposits on the neural membranes, with larger deposits and neuritic plaques forming later in the disease [11]. Aβ isolated from human brain varies in reported distributions of monomer, dimer, trimer, tetramer and higher-order oligomers [11]. Aβ oligomers have been identified in conditioned media of certain cell lines that constitutively secrete Aβ [10,18] and as components of cerebrospinal fluid [19]. As well as low-molecular-mass oligomers, protofibrils, sizeable ($>100\,000$ kDa) oligomeric structures that lack the repeating structure of fibrils, have been identified as products of aged Aβ solutions [9,20,21].

In the present studies, E22Q or native Aβ in freshly prepared solutions were eluted as symmetrical peaks with elution times of 34.6 min from a column of Superdex 75 (Figure 2), a time that was not altered by preincubation of Aβ in the disaggregating solvents formic acid, DMSO or hexafluoroisopropanol [22], indicating that 34.6 min is the elution time of the monomer. After 1 h preincubation of the Aβ peptides, changes in the elution profiles were found, indicative of formation of higher-molecular-mass oligomers. Other authors have suggested that dimers exist in Aβ solutions under most aqueous conditions [11,12,21]. The characterization of dimers in previous studies rested on the behaviour of Aβ solutions on gel-filtration columns, on SDS/PAGE or in quasi-light-scattering spectroscopy (QLS), studies which required calibration with standard small proteins of known molecular mass [21,23]. However, small proteins of molecular mass similar to that of Aβ are not eluted in positions that accord to their molecular mass from Superdex 75 columns (Table 1). In particular, neuropeptide Y (4.2 kda) and bovine aprotinin (molecular mass 6.5 kDa) are much more strongly retarded on the column than other peptides and proteins of lower molecular mass. It seems likely that elution behaviour is more strongly influenced by the composition and degree of folding of the peptides than their molecular size. Similar conclusion were

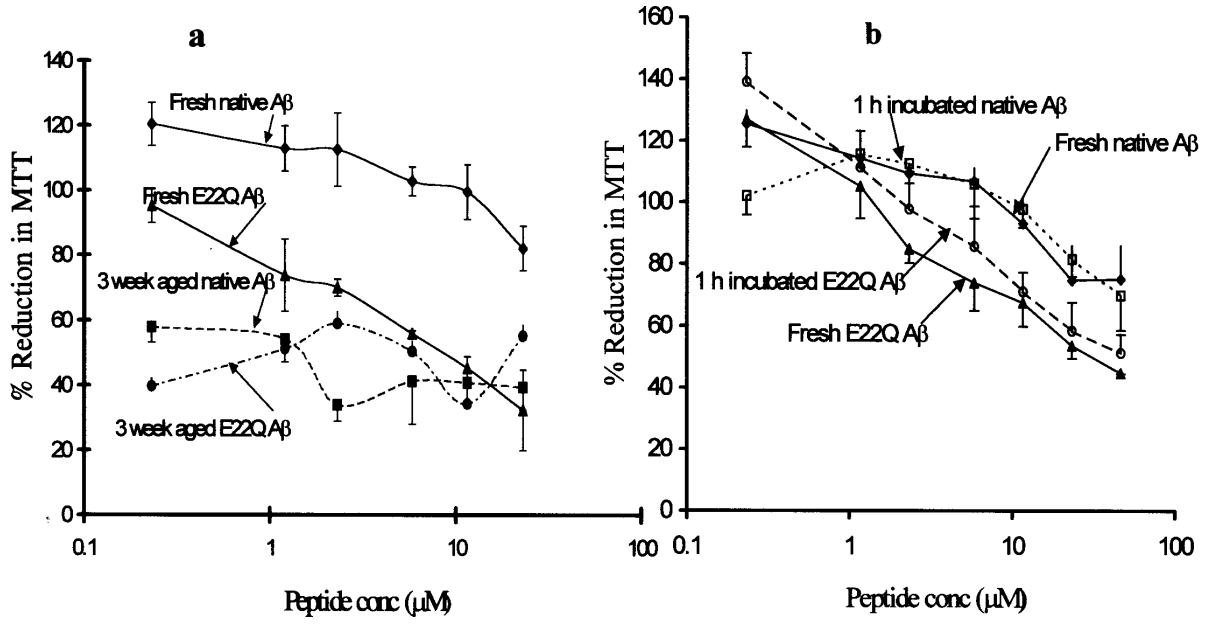

Figure 6 Cytotoxic effect of aged and fresh Aβ peptides

Shown is a comparison of the ability to reduce MTT by SH-SY5Y cells incubated for 48 h with freshly prepared native Aβ (---◆---) or E22Q Aβ (---▲---) (**a** and **b**) and aged (3 weeks) native Aβ (––■––) and E22Q Aβ (---●---) solutions (**a**) or 1 h preincubated solutions of native Aβ (––□––) and E22Q Aβ (––○––) (**b**) (preincubated at 1.16 mM and diluted into the media surrounding the cells. Data shown are expressed as percentage of control values (no peptides). Under the same conditions, camptothecin incubated with the cells led to a reduction in MTT staining of 93%. S.E.M. values for assays performed in triplicate are shown for each point as bars above and/or below the mean.

reached by others [24] who found that Aβ was not eluted as expected from a size-exclusion column calibrated with a wide range of globular proteins. These workers also found, by translational diffusion measurements using NMR, that Aβ behaves as monomers in solution. Moreover, its elution behaviour did not allow one to differentiate whether Aβ exists as an extended monomer or a compact dimer [25].

Evidence for Aβ dimers in solution has come from studies of size-exclusion chromatography in salt. High salt has previously been found to precipitate Aβ, leaving a small percentage of a species that is eluted from a column of Bio-Gel P10 as a monomer, whereas, under most other aqueous conditions, Aβ has a reduced elution time, possibly behaving as a dimer [23]. Inclusion of NaF in the elution buffer caused Aβ to be eluted later from Bio-Gel P10. However, as NaF also significantly altered the behaviour of the standard proteins used [23], the changes observed in elution behaviour of Aβ were difficult to interpret. QLS measurements made on Aβ solutions were also suggestive of dimers, but QLS is known to be less useful in studying small molecules when they exist in equilibrium with polymers [21].

An ELISA was developed to probe the oligomeric nature of native and E22Q Aβ. The formation of additional epitopes to the N-terminal specific antibody anti-NTA4 in oligomers attached to the wells by one epitope via immobilized non-biotinylated anti-NTA4 were detected by an increase in binding to a biotinylated form of the same antibody (Figure 1). The increases in binding to biotinylated-anti-NTA4 in incubated solutions of the Aβ peptides indicate that soluble oligomeric species are generated from the initially monomeric species over the course of incubation. The possibility that the fresh solutions already contain dimers in which the epitopes are so close that they cannot simultaneously bind the non-biotinylated and biotinylated forms of the anti-NTA4 antibody cannot, however, be excluded. The maximum increases in absorbance from ELISA occurred under conditions of incubation similar to those that gave rise to a decrease in the elution time (of 1.6 min) to the major peak eluted from Superdex 75, and to the appearance of shoulders on this peak (Figure 2), supporting the contention that oligomers are formed from monomers during incubation. E22Q Aβ formed oligomers, detected by the increase in biotinylated anti-NTA4 binding, more rapidly than native Aβ. Soluble protofibrils, which are eluted in the void volume from Superdex 75, in 18 h incubates of native Aβ and 60 min incubates of E22Q Aβ were also seen (Figure 2; [9]). As a control, solutions of the N-terminal ten-residue peptide, which does not contain the sequences known to be important for oligomerization [23], but contains the complete epitope for the antibody anti-NTA4 [15], did not show increased binding to the antibody upon incubation.

The binding to biotinylated-anti-NTA4 of oligomers produced in solutions of E22Q Aβ incubated at 1.16 mM and 0.116 mM reached a maximum, and then declined at a low rate, which was commensurate with the appearance of insoluble fibrils. The most likely cause of the decline is a slow occlusion of some of the binding sites to anti-NTA4 by precipitation of insoluble fibrils. In contrast, native Aβ did not show any decline in binding with incubations of up to 24 h, and did not yield fibril precipitates until after several days of aging. In keeping with these results observed on 1–40 full-length amyloid peptides, fragments 13–26 and 1–28 of E22Q mutation in Aβ have been reported to fibrillize more rapidly that fragments of native Aβ [26,27]. An ELISA similar in principle has been described [28] for the detection of inhibitors of Aβ fibrillization.. However, the changes occurring with time during incubation of Aβ peptides were not studied, and insufficient detail is given [28] to compare sensitivities of the assays.

The formation of soluble oligomers measured by ELISA was found to be dependent on the concentrations of the incubated Aβ

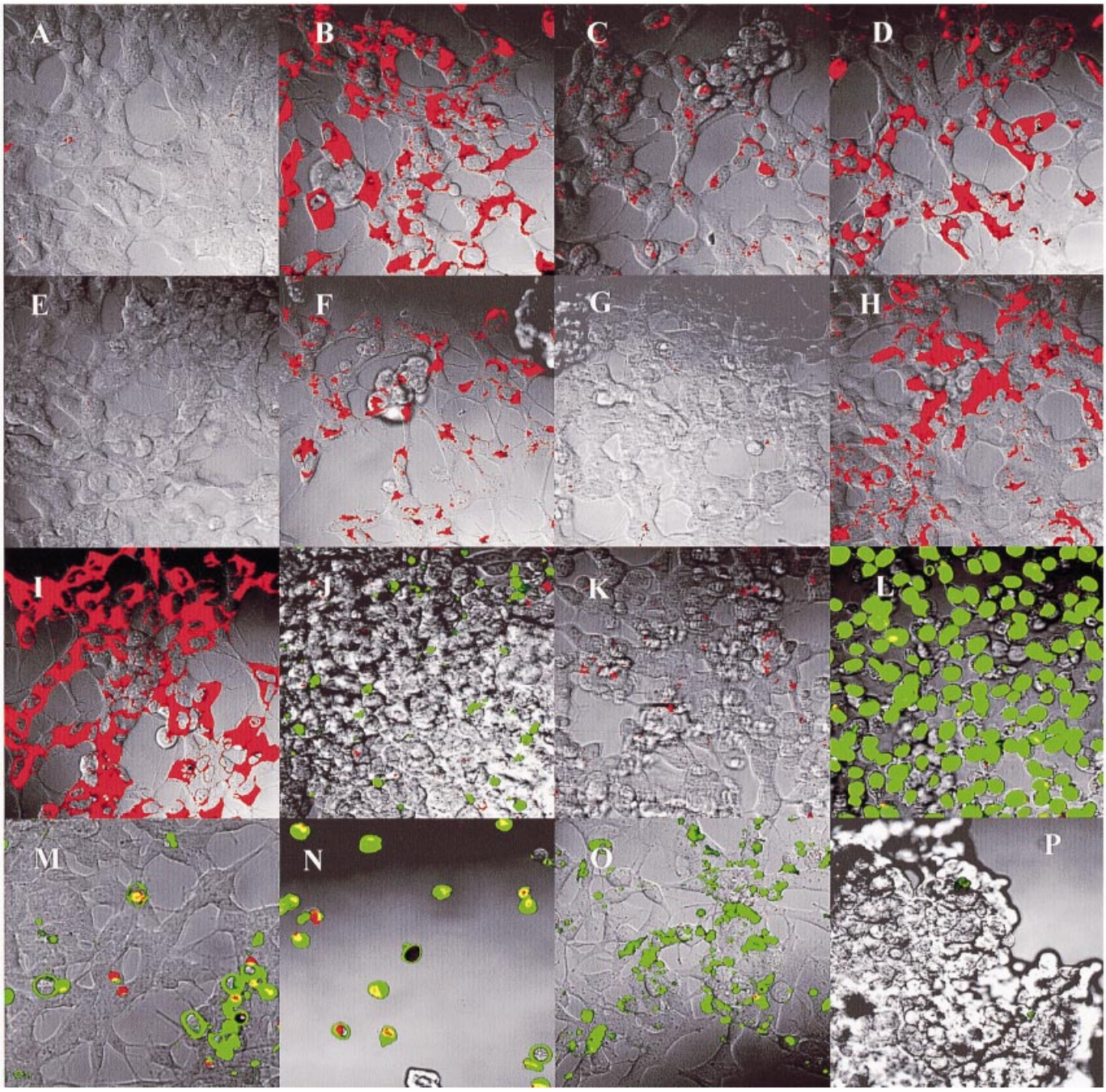

Figure 7 Apoptotic effects of native and E22Q Aβ peptides

Representative fluorescence photomicrographs showing the loss of mitochondrial membrane potential monitored by loss of CMXRos (red) fluorescence (**A**–**L**) or the appearance of phosphatidylserine monitored by binding with annexin V conjugated to Alexa 488 (green fluorescence) (**M**–**P**) in SHSY-5Y cells treated with aged (3 weeks) (**A**, **C** and **M**) or fresh (**B** and **D**) preparations of native Aβ, or aged (**E**, **G** and **N**) or fresh (**F** and **H**) preparations of E22Q Aβ. Peptides were incubated with cells at 11.6 μM (**A**, **B**, **E**, **F**, **M** and **N**) or 2.3 μM (**C**, **D**, **G** and **H**) for 10 h. Apoptosis induced by camptothecin is shown at 15 μM in (**J**) and 50 μM in (**K**) and (**O**), and necrosis induced by H_2O_2 is shown in (**L**). Control cells (no additions) are shown in (**I**) and (**P**). Sytox (green) (**A**–**L**) or propidium iodide (red) (**M**–**P**) detected any necrotic cells. Cells are outlined in grey as differential contrast interference images.

peptides (Figure 1). In contrast, fluorescence resonance energy transfer observed from DMSO solutions of fluorescently labelled Aβ diluted into aqueous buffers did not change over concentrations from 3 μM to 100 nM [11]. It is possible that oligomers formed from modified fluorescent peptides give rise to much more stable dimers than those of unmodified Aβ. Alternatively, the use of organic solvents [11] may have had marked effects on the behaviour of the Aβ adducts [22].

The conversion of random to β-sheet conformation of native and E22Q Aβ peptides detected by CD were an order of magnitude lower than rates at which soluble low-molecular-mass oligomers, detected by ELISA and gel filtration, are formed

(Figure 3). In the association process, Aβ molecules may be driven together in a way that retains their irregular structure, and then undertake slower conformational transitions into β-sheets in ways which are very sensitive to the amino acid change E22Q. The molecular changes that take place during the initial stages of oligomerization are clearly important in determining the kinetics and equilibrium of the fibrillar product, although precipitation of fibrils may be dependent upon a nucleation process [29]. X-ray-diffraction measurements of fibrils formed by Aβ1–28 indicated that residues LVFF$^{17-20}$ form a hydrophobic core in the fibrils [30]. The marked changes observed in the 250–288 nm region (Figure 3), associated with changes in the CD contributions of the side chains Phe^{19} and Phe^{20}, concur with the interpretations of X-ray data. A change in the environment of the Phe residues upon oligomerization is consistent with the results of peptide scanning [31,32], which showed that KLVFF$^{16-20}$ is a sequence in Aβ essential for fibril formation which efficiently binds to the total Aβ sequence.

Previous comparisons of the CD of 1–42 versions of these two peptides showed that, in 50% acetonitrile, the E22Q sequence has a higher percentage of β-sheet than the native 1–42 [33]. These findings are here extended to show that the E22Q mutation plays an important role in altering the rates of oligomerization and random-coil-to-β-sheet transition in Aβ, and conformational changes occurring during pH change. Molecular modelling of Aβ 14–23 previously suggested that favourable hydrophobic interactions are stabilized by salt bridges between the two Aβ strands arranged anti-parallel [34]. Involvement of E22 in a stabilizing salt bridge would not account for the more rapid rate of oligomerization and fibrillization found in E22Q Aβ. The distances between isotopically labelled carbonyl carbon atoms of Gln^{15} and Lys^{16} in adjacent strands, measured by solid-state NMR to be 5.1 ± 0.2 and 4.9 ± 0.2 Å respectively, suggest that Aβ strands are aligned in a parallel β-strand with residues in register [35]. Parallel, in-register β-sheet formation is consistent with the strong 5 Å and weak 10 Å angstrom X-ray-diffraction reflections seen in fibrils [30]. An energy-minimized molecular model showing the dimeric arrangement of residues 15–22 in native and E22Q Aβ peptides (Figure 4) would satisfy these carbonyl carbon distances. Additional hydrogen bonding between Gln^{22} residues, and lack of charge repulsion between Glu^{22} side chains, would explain why E22Q Aβ oligomers form more rapidly than native Aβ.

There is increasing evidence that apoptosis plays a role in neuronal cell death in neurodegenerative disease. For example, neurons in post-mortem specimens from Alzheimer's patients show DNA damage and increased c-Jun immunoreactivity in the enterorhinal cortex [36]. Fibril-containing suspensions of native and E22Q Aβ produced by incubation at high concentrations for 3 weeks were more active than freshly prepared solutions in reducing MTT uptake (Figure 6) or inducing apoptotic changes (Figure 7), by further incubation at low concentrations with SHSY-5Y cells for 72 h (Figure 6) or 10 h (Figure 7). In contrast, there were no differences in the MTT reduction induced between freshly prepared solutions and solutions of high concentrations of native or E22Q Aβ incubated for 1 h (Figure 6). Thus fibrils are far more apoptotic and toxic than the low-molecular-mass oligomers produced in a 1 h incubation (Figures 1 and 2). The toxicity of low-molecular-mass oligomers reported previously may have been due to conversion into fibrils over the 5-day incubation period with the cells in culture [9].

Aged E22Q preparations are far more potent in inducing apoptotic changes and reducing MTT uptake than equal concentrations of aged native Aβ preparations (Figures 6 and 7). Toxicity differences may be due to the characteristic morphology of the fibrils formed [37]; the E22Q fibrils are short and stubby in appearance, whereas those formed by native Aβ are long and spindly (Figure 5). The different morphologies of the fibrils of native and E22Q Aβ peptides have been noted previously [38], although X-ray diffraction measurements of native and E22Q Aβ fibrils indicate they are both of similar crossed β-sheet structure. An E22K mutation in two Italian families apparently produces clinical and pathological findings highly similar to those of the E22Q Dutch disease [39], consistent with the notion that the clinical manifestations of the Dutch mutation are due to the molecular consequences of the replacement of Glu^{22}. In contrast with neuronal cell types, human cerebrovascular smooth-muscle cells are not killed by fully fibrillized forms of native Aβ 1–42 or E22Q Aβ [40], whereas E22Q Aβ 1–40 added in its soluble forms to these cells is highly toxic [41]. These differential effects towards different cell types may in part explain the differential pathology of HCHWA-D and AD. Modelling studies *in vitro* suggest that the propensity of E22Q to form fibrils could result in increased fibril binding to vascular-wall components, such as heparin, which would accelerate vascular amyloid deposition [4]. Furthermore, E22Q Aβ 1–40, but not wild-type Aβ 1–40, has been found to cause cellular degeneration into fibrils assembled *in situ* on smooth-muscle-cell surfaces, [41]. Degeneration has been observed in cultured brain pericytes treated with the Dutch E22Q Aβ [42]; in each case, fibril assembly was a prerequisite for toxicity. Elucidation of the molecular events which initiate oligomerization, a necessary intermediate step in the fibrillization process, are crucial to understanding the pathology and to developing potential therapeutics, not only of AD, but also for strokes caused by amyloidogenesis in cerebral vascular cell walls.

We are grateful to Research into Ageing, CeNeS plc and the Engineering and Physical Science Research Council for their support, and Mr R. Moss in the Electron Microscopy Unit at St George's Hospital for the electron micrographs.

REFERENCES

1 Muller-Hill, B. and Beyreuther, K. (1989) Molecular biology of Alzheimer's disease. Annu. Rev Biochem. **58**, 287–307
2 Haan, J. Algra, P. R. and Roos, R. A. C. (1990) Hereditary cerebral hemorrhage with amyloidosis-Dutch type. Clinical and computed tomographic analysis of 24 cases. Arch. Neurol. **47**, 649–653
3 Maat-Schieman, M. L., van Duinen, S. G., Rozemuller, A. J., Haan, J. and Roos, R. A. (1994) Hereditary cerebral hemorrhage with amyloidosis (Dutch): a model for congophilic plaque formation without neurofibrillary pathology. Acta Neuropathol. **88**, 371–378
4 Watson, D. J., Selkoe, D. J. and Teplow, D. B. (1999) Effects of the amyloid precursor protein Glu^{693} → Gln 'Dutch' mutation on the production and stability of amyloid β-protein. Biochem. J. **340**, 703–709
5 Pike, C. J., Burdick, A. J., Walencewicz, C. G., Glabe, C. G. and Cotman, C. W. (1993) Neurodegeneration induced by β-amyloid peptides *in vitro*: the role of peptide assembly state. J. Neurosci. **13**, 1676–1687
6 Lorenzo, A. and Yankner, B. A. (1994) Beta-amyloid neurotoxicity requires fibril formation and is inhibited by congo red. Proc. Natl. Acad. Sci. U.S.A. **91**, 12242–12247
7 Mattson, M. P., Tomaselli, K. J. and Rydel, R. E. (1993) Calcium-destabilizing and neurodegenerative effects of aggregated beta-amyloid peptide are attenuated by basic FGF. Brain Res. **621**, 35–49
8 Younkin, S. G. (1998) The role of A beta 42 in Alzheimer's disease. J. Physiol. (London) **92**, 289–292
9 Hartley, D. M., Walsh, D. M., Ye, C. P., Diehl, T., Vassilev, P. M., Teplow, D. B. and Selkoe, D. J. (1999) Protofibrillar intermediates of amyloid beta-protein induce acute electrophysiological changes and progressive neurotoxicity in cortical neurons. J. Neurosci. **19**, 8876–8884
10 Podlisny, M. B., Ostaszewski, B. L., Squazzo, S. L., Koo, E. H., Rydell, R. E., Teplow, D. B. and Selkoe, D. J. (1995) Aggregation of secreted amyloid beta-protein into sodium dodecyl sulfate-stable oligomers in cell culture. J. Biol. Chem. **270**, 9564–9570

11 Roher, A. E., Chaney, M. O., Kuo, Y. M., Webster, S. D., Stine, W. B., Haverkamp, L. J., Woods, A. S., Cotter, R. J. et al. (1996) Morphology and toxicity of Aβ-(1–42) dimer derived from neuritic and vascular amyloid deposits of Alzheimer's disease. J. Biol. Chem. **271**, 20631–20635

12 Garzon-Rodriguez, W., Sepulveda-Becerra, M., Milton, S. and Glabe, C. G. (1997) Soluble amyloid Aβ-(1–40) exists as a stable dimer at low concentrations. J. Biol. Chem. **272**, 21037–21044

13 Funato, H., Enya, M., Yoshimura, M., Morishima-Kawashima, M. and Ihara, Y. (1999) Presence of sodium dodecyl sulfate-stable amyloid beta-protein dimers in the hippocampus CA1 not exhibiting neurofibrillary tangle formation. Am. J. Pathol. **155**, 23–28

14 El-Agnaf, O. M. A., Goodwin, H., Sheridan, J. M., Frears, E. R. and Austen, B. M. (1999) Improved solid-phase synthesis of amyloid proteins associated with neurodegenerative diseases. Pep. Protein Lett. **7**, 1–8

15 Stephens, D. J. and Austen, B. M. (1996) Metabolites of the beta-amyloid precursor protein generated by beta-secretase localise to the trans-Golgi network and late endosome in 293 cells. J. Neurosci. Res. **45**, 211–225

16 El-Agnaf, O. M. A., Jakes, R., Curran, M. D., Middleton, D., Ingenito, R., Bianchi, E., Pessi, A., Neill, D. and Wallace, A. (1998) Aggregates from mutant and wild-type alpha-synuclein proteins and NAC peptide induce apoptotic cell death in human neuroblastoma cells by formation of beta-sheet and amyloid-like filaments. FEBS Lett. **440**, 71–75

17 Denziot, F. and Lang, R.. (1986) Rapid colorimetric assay for cell growth and survival. Modifications to the tetrazolium dye procedure giving improved sensitivity and reliability. J. Immunol. Methods **89**, 271–277

18 Xia, W., Zhang, J., Kholodenko, D., Citron, M., Podlisny, M. B., Teplow, D. B., Haas, C., Seubert, P., Koo, E. H. and Selkoe, D. J. (1997) Enhanced production and oligomerization of the 42-residue amyloid beta-protein by Chinese hamster ovary cells stably expressing mutant presenilins. J. Biol. Chem. **272**, 7977–7982

19 Pitschke, M., Prior, R., Haupt, M. and Riesner, D. (1998) Detection of single amyloid beta-protein aggregates in the cerebrospinal fluid of Alzheimer's patients by fluorescence correlation spectroscopy. Nat. Med. **4**, 832–834

20 Harper, J. D., Wong, S. S., Lieber, C. M. and Lansbury, P. T. (1997) Observation of metastable Abeta amyloid protofibrils by atomic force microscopy. Chem. Biol. **4**, 119–125

21 Walsh, D. M., Lomarkin, A., Benedek, G. B., Condron, M. M. and Teplow, D. B. (1997) Amyloid beta-protein fibrillogenesis. Detection of a protofibrillar intermediate. J. Biol. Chem. **272**, 22364–22372

22 Snyder, S. W., Ladror, U. S., Wade, W. S., Wang, G. T., Barrett, L. W., Matayoshi, E. D., Huffaker, H. J., Krafft, G. A. and Holzman, T. F. (1994) Amyloid-beta aggregation: selective inhibition of aggregation in mixtures of amyloid with different chain lengths. Biophys. J. **67**, 1216–1228

23 Hilbich, C., Kisters-Woike, B., Reed, J., Masters, C. L. and Beyreuther, K. (1991) Aggregation and secondary structure of synthetic amyloid beta A4 peptides of Alzheimer's disease. J. Mol. Biol. **218**, 149–163

24 Tseng, B. P., Esler, W. P., Clish, C. B., Stimson, E. R., Ghilardi, J. R., Vinters, H. V., Mantyh, P. W., Lee, J. P. and Maggio, J. E. (1999) Deposition of monomeric, not oligomeric, Aβ mediates growth of Alzheimer Disease amyloid plaques in human brain preparations. Biochemistry **38**, 633–642

25 Walsh, D. M., Hartley, D. M., Kusumoto, Y., Fezouli, Y., Condron, M. M., Lomakin, A., Benedek, G. B., Selkoe, D. J. and Teplow, D. B. (1999) Amyloid β-protein fibrillogenesis; structure and biological function of protofibrillar intermediates. J. Biol. Chem. **274**, 25945–25952

26 Clements, A., Walsh, D. M., Williams, C. H. and Allsop, D. (1993) Effects of the mutations Glu22 to Gln and Ala21 to Gly on the aggregation of a synthetic fragment of the Alzheimer's amyloid beta/A4 peptide. Neurosci. Lett. **161**, 17–20

27 Wisniewski, T., Ghiso, J. and Frangione, B. (1991) Peptides homologous to the amyloid protein of Alzheimer's disease containing a glutamine for glutamic acid substitution have accelerated amyloid fibril formation. Biochem. Biophys. Res. Commun. **179**, 1247–1254

28 Howlett, D., Cutler, P., Heales, S. and Cammilleri, P (1997) Hemin and related porphyrins inhibit β-amyloid aggregation. FEBS. Lett. **417**, 249–251

29 Lomakin, A., Teplow, D. B., Kirschner, D. A. and Beneder, G. B. (1997) Kinetic theory of fibrillogenesis of amyloid beta-protein. Proc. Natl. Acad. Sci.. U.S.A. **94**, 7942–7947

30 Inouye, H. and Kirschner, D. A. (1996) The Nature and Origin of Amyloid Fibrils, pp. 22–38, Wiley, Chichester

31 Tjernberg, L. O., Naslund, J., Lindqvist, F., Johansson, J., Karlstrom, A. R., Thyberg, J., Terenius, L. and Nordstedt, C. (1996) Arrest of beta-amyloid fibril formation by a pentapeptide ligand. J. Biol. Chem. **271**, 8545–8548

32 El-Agnaf, O. M. A., Guthrie, D. J. S., Walsh, D. M. and Irvine, G. B. (1998) The influence of the central region containing residues 19–25 on the aggregation properties and secondary structure of Alzheimer's beta-amyloid peptide. Eur. J. Biochem. **256**, 560–569

33 Fabian, H., Szendrei, G. I., Mantsch, H. H. and Otvos, L. (1993) Comparative analysis of human and Dutch-type Alzheimer beta-amyloid peptides by infrared spectroscopy and circular dichroism. Biochem. Biophys. Res. Commun. **191**, 232–239

34 Tjernberg, L. O., Callaway, D. J. E., Tjernberg, A., Hahne, S., Lilliehook, C., Terenius, L., Thyberg, J. and Nordstedt, C. (1999) A molecular model of Alzheimer amyloid beta-peptide fibril formation. J. Biol. Chem. **274**, 12619–12625

35 Benzinger, T. L. S., Gregory, D. M., Burkoth, T. S., Miller-Auer, H., Lynn, D. G., Botto, R. E. and Meredith, S. C. (1998) Propagating structure of Alzheimer's beta-amyloid(10–35) is parallel beta-sheet with residues in exact register. Proc. Natl. Acad. Sci. U.S.A. **95**, 13407–13412

36 Anderson, A. J., Su, J. H. and Cotman, C. W. (1996) DNA damage and apoptosis in Alzheimer's disease: colocalization with c-Jun immunoreactivity, relationship to brain area, and effect of postmortem delay. J. Neurosci. **16**, 1710–1719

37 Seilheimer, B., Bohrmann, B., Bondolfi, L., Muller, F., Stuber, D. and Dobeli, H. (1997) The toxicity of the Alzheimer's beta-amyloid peptide correlates with a distinct fiber morphology. J. Struct. Biol. **119**, 59–71

38 Fraser, P. E., Nguyen, J. T., Inouye, H., Surewicz, W. K., Selkoe, D. J., Podlisny, M. B. and Kirschner, D. A. (1992) Fibril formation by primate, rodent, and Dutch-hemorrhagic analogues of Alzheimer amyloid beta-protein. Biochemistry **31**, 107161–10723

39 Bugiani, O., Padovani, A., Magoni, M., Andora, G., Sgarzi, M., Savoiardo, M., Bizzi, A., Giaccone, G., Rossi, G. and Tagliavini, F. (1998) An Italian type of HCHWA. Neurobiol. Aging **19**, S23

40 Davis, J. and van Nostrand, W. E. (1996) Enhanced pathologic properties of Dutch-type mutant amyloid beta-protein. Proc. Natl. Acad. Sci. U.S.A. **93**, 2996–3000

41 van Nostrand, W. E., Melchor, J. P. and Ruffinini, L. (1998) Pathologic amyloid beta-protein cell surface fibril assembly on cultured human cerebrovascular smooth muscle cells. J. Neurochem. **70**, 216–223

42 Verbeek, M. M., Dewaal, R. M. W., Schipper, J. J. and van Nostrand, W. E. (1997) Rapid degeneration of cultured human brain pericytes by amyloid beta protein. J. Neurochem. **68**, 1135–1141

Received 4 January 2000/13 March 2000; accepted 3 April 2000